

Functional analysis of the novel mycorrhiza-specific phosphate transporter AsPT1 and PHT1 family from *Astragalus sinicus* during the arbuscular mycorrhizal symbiosis

Xianan Xie^{1,2}, Wu Huang^{1,2}, Fengchuan Liu^{1,2}, Nianwu Tang^{1,2}, Yi Liu^{1,2}, Hui Lin^{1,2} and Bin Zhao^{1,2}

¹State Key Laboratory of Agricultural Microbiology, Huazhong Agricultural University, Wuhan Hubei, 430070, China; ²College of Life Science and Technology, Huazhong Agricultural University, Wuhan Hubei, 430070, China

Summary

Authors for correspondence:

Bin Zhao

Tel: +86 27 87281809

Email: binzhao@mail.hzau.edu.cn

Hui Lin

Tel: +86 27 87281809

Email: linhui@mail.hzau.edu.cn

Received: 29 November 2012

Accepted: 14 January 2012

New Phytologist (2013) **198**: 836–852

doi: 10.1111/nph.12188

Key words: arbuscular mycorrhizas, AsPT1, AsPT4, *Astragalus sinicus*, overexpression, Pht1 family, RNA interference.

- Arbuscular mycorrhizas contribute significantly to inorganic phosphate (Pi) uptake in plants. Gene networks involved in the regulation and function of the Pht1 family transporters in legume species during AM symbiosis are not fully understood.
- In order to characterize the six distinct members of Pht1 transporters in mycorrhizal *Astragalus sinicus*, we combined cellular localization, heterologous functional expression in yeast with expression/subcellular localization studies and reverse genetics approaches in planta. *Pht1;1* and *Pht1;4* silenced lines were generated to uncover the role of the newly discovered dependence of the AM symbiosis on another phosphate transporter AsPT1 besides AsPT4.
- These Pht1 transporters are triggered in Pi-starved mycorrhizal roots. *AsPT1* and *AsPT4* were localized in arbuscule-containing cells of the cortex. The analysis of promoter sequences revealed conserved motifs in both *AsPT1* and *AsPT4*. *AsPT1* overexpression showed higher mycorrhization levels than controls for parameters analysed, including abundance of arbuscules. By contrast, knockdown of *AsPT1* by RNA interference led to degenerating or dead arbuscule phenotypes identical to that of *AsPT4* silencing lines. *AsPT4* but not *AsPT1* is required for symbiotic Pi uptake.
- These results suggest that both, *AsPT1* and *AsPT4*, are required for the AM symbiosis, most importantly, *AsPT1* may serve as a novel symbiotic transporter for AM development.

Introduction

Arbuscular mycorrhiza (AM) is a mutualistic endosymbiotic association between fungi of the ancient phylum Glomeromycota and most vascular land plant species (Remy *et al.*, 1994). More than 80% of terrestrial plant species are known to be able to form AM symbiosis (Denison & Kiers, 2011). This mutualism improves the plant's efficiency for uptake of mineral nutrients, particularly phosphates, and in return fungi obtain organic carbon from the plant to complete the fungal life cycle (Smith & Read, 2008). To form AM symbiosis, the two symbionts undergo a series of developmental transitions that enable the fungus to enter the root cortex and establish highly dichotomously branched arbuscules in which phosphate and other nutrients are delivered to the root (Bucher, 2007). During arbuscule development, a plant-derived membrane, the peri-arbuscular membrane (PAM) develops around the branching hypha and separates the fungus from the plant cell cytoplasm. Phosphate transport proteins essential for symbiotic inorganic phosphate (Pi) transfer to the plant cell reside in this membrane (Harrison *et al.*, 2002). Symbiotic phosphate transport in AM plants is mediated by

specific phosphate transporters (Karandashov & Bucher, 2005). Phosphorus (P), as an essential mineral nutrient, plays a key role in AM symbiosis. Because of phosphate's low mobility and thus its availability in soil (Ai *et al.*, 2009), plants adopt a series of adaptive strategies to increase the acquisition of poorly available Pi. One of them is the formation of symbiosis with AM fungi.

Plant Pht1 transporters belong to the phosphate: H⁺ symporter (PHS) family within the major facilitator superfamily (MFS; Pao *et al.*, 1998). So far, Pht1 transporters in the direct uptake pathway occurring through the epidermal cells have been observed in potato (StPT1 and StPT2; Rausch *et al.*, 2001); *Medicago truncatula* (MtPT1 and MtPT2; Liu *et al.*, 1998b); rice (OsPT1-10; Paszkowski *et al.*, 2002); and barley (HvPT1 and HvPT2; Rae *et al.*, 2003). AtPHR1 and OsPHR2 are key regulators in the Pi signalling pathway (Jia *et al.*, 2011), and overexpression of the two genes results in excessive accumulation of Pi in shoots, and upregulation of the Pht1 genes under Pi-sufficient conditions (Liu *et al.*, 2010). Currently, only a few of these Pi transporters have been functionally characterized. The double *pht1;1* and *pht1;4* mutant from *Arabidopsis thaliana* exhibits a significant decrease in Pi uptake and shoot accumulation under both

Pi-sufficient and Pi-deficient conditions, indicating compensatory effects between the two transporters (Shin *et al.*, 2004), and AtPht1;5 plays a critical role in mobilizing Pi from source to sink organs in accordance with the P status of the plant (Nagarajan *et al.*, 2011). The fourth Pht1 member functionally characterized so far, AtPht1;9 transporter, mediates root Pi acquisition under Pi-deprived conditions, contributing to the overall plant Pi status (Remy *et al.*, 2012).

Several mycorrhiza-specific Pht1 members have been identified in *M. truncatula* (MtPT4), rice (OsPT11), potato (StPT4 and StPT5) and tomato (SlPT4) (Harrison *et al.*, 2002; Paszkowski *et al.*, 2002; Nagy *et al.*, 2005; Chen *et al.*, 2007; Xu *et al.*, 2007). Tissue localization studies revealed that the mycorrhiza-induced Pht1 genes are exclusively expressed in arbuscule-containing cells (Harrison *et al.*, 2002). The spatial expression pattern of these genes suggests that a cell autonomous signal involved in arbuscule development, activates expression of these genes (Gomez-Ariza *et al.*, 2009). Lysophosphatidylcholine (LPC) may be one of these signals, as it was shown to trigger mycorrhiza specific Pi transporter gene expression in potato and tomato (Drissner *et al.*, 2007). Functional analysis of these Pi transporter promoters revealed that PIBS and MYCS elements are required to confer the AM-inducible PiT gene expression (Chen *et al.*, 2011). MtPT4 is essential for symbiotic Pi transport and the development of AM symbiosis (Javot *et al.*, 2007b). The mycorrhiza-inducible Pi transporters StPT3, StPT4 and StPT5 from potato, exhibit functional redundancy (Nagy *et al.*, 2005). Knockdown of *LjPT3* exhibits a decrease in *Glomus mosseae* arbuscules and necrotic root nodules (Maeda *et al.*, 2006). However, the functions of other mycorrhiza-specific Pi transporters have not been described.

Here, we report on the characterization of two novel mycorrhiza-specific Pi transporters, AsPT1 and AsPT4, and four other Pht1 family members from *Astragalus sinicus*, designated as AsPT2, AsPT3, AsPT5 and AsPT6, respectively. Both AsPT1 and AsPT4 play critical roles during the development of AM symbiosis, but AsPT4 alone is required for symbiotic Pi uptake.

Materials and Methods

Plant materials, AM fungi inoculum and cultivation conditions

Astragalus sinicus L. was used in this study. Seeds were surface sterilized and then spread on 0.8% water agar plates for germination. In pot culture (Expt 1), the plantlets were adapted to glasshouse conditions (see Supporting Information Methods S1) for 7 d first, and then, an equal number of plants were transferred either to pots containing a soil : sand mixture (v/v, 1 : 2), or to pots containing the same mixture supplemented with roots of *Astragalus sinicus* colonized with *Gigaspora margarita* (BEG34) or *Glomus intraradices* (BEG141). All plants were supplied with Hoagland's nutrient solution containing the macro- and micronutrients (see Methods S1). The experiment comprised three replicates for each treatment. Plants were harvested at 4 wk post-inoculation (wpi). The freshly collected roots were washed with

deionized water and part of the roots were immediately frozen in liquid nitrogen and stored at -70°C for subsequent RNA isolation. Other parts of the roots were used to evaluate colonization and for visualization of arbuscules.

Monoxenic AM cultures

In monoxenic culture (Expt 2), the AM fungus *G. margarita* or *G. intraradices* was grown monoxenically in mycorrhizal association with hairy roots of *A. sinicus*. The cultures are clones of *A. sinicus* roots that were initially transformed using *Agrobacterium rhizogenes* K599 as transformation system with the T-DNA of the root-inducing plasmid transferred to the plant genome (Boisson-Dernier *et al.*, 2001; Li *et al.*, 2008). AM-colonized cultures were maintained at a constant temperature of 26°C on petri dishes with 0.3% (w/v) Phytigel (Sigma-Aldrich) as the gelling agent and with MSR medium containing 3% sucrose as the C source and $30\ \mu\text{M}$ Pi (as $6.41\ \text{mg}\ \text{KH}_2\text{PO}_4\ \text{l}^{-1}$).

Cloning of the Pi transporter genes

Based on the conserved amino acid sequences of legume plant Pi transporters (Harrison *et al.*, 2002), we designed the following degenerate oligonucleotides: forward (AsPTF, 5'-TTCWGGYT YKGVYTYGGMWYGG-3', which encodes FRFWLGF; and reverse (AsPTR), 5'-TTVGGVCCRAAVTTSGCRAAGAAG-3', which is antisense for FFFANFGP. Subsequent PCRs on the total DNA from *A. sinicus* resulted in 850–900 bp amplified DNA segments encoding six putative Pi transporters, named *AsPT1* through *AsPT6*.

The 5' and 3' regions of these putative Pi transporter genes, were cloned via thermal asymmetric interlaced PCR (TAIL-PCR), inverse PCR (iPCR) and RACE. For TAIL-PCR, four relatively longer AD (LAD) primers of 33 or 34 nucleotides were designed (Liu & Chen, 2007). For iPCR, 3–5 μg genomic DNA isolated from *A. sinicus* were digested with *EcoRI*, *KpnI*, *BamHI*, *NcoI* or *HindIII*, then self-ligated and used for PCR. The 5' RACE and 3' RACE were carried out using the classic RACE protocols (Scotto-Lavino *et al.*, 2006a,b). For the primers used, see Table S1.

RNA extraction, cDNA synthesis, RT-PCR and real-time RT-PCR

Total RNA was extracted from *A. sinicus* by Trizol reagents (Invitrogen) following the manufacturer's instructions. After treatment with DNase I (MBI Fermentus, Canada), the 1st cDNA strand for each RNA preparation was synthesized by using oligo (dT)₁₈ and Reverse Transcriptase M-MLV (RNase H⁻) (TaKaRa, Dalian, China). RT-PCR was performed as the manufacturer's instructions, using gene-specific primers (Table S1). Real-time PCR was performed using the SYBR Green Master Mix (Toyobo, Japan), and then subjected to qPCR reactions according to the manufacturer's instructions using an Applied Biosystems Cyclor System (Applied Biosystems, CA, USA). The gene-specific primers are listed in Table S1. All reaction mixtures

were heated at 95°C for 30 s, and then subjected to 40 PCR cycles of 95°C for 20 s, 60°C for 20 s and 72°C for 20 s, with the resulting fluorescence being monitored. All the reactions were performed with three biological replicates, each with three technical replications. The relative quantity (RQ) was determined using the Cyclor system with software; the data were analysed using the $2^{-\Delta\Delta C_T}$ method.

AsPT1, *AsPT4* and *AsPT5* promoter-*Uida* constructs

The isolated fragments of the *AsPT1*, *AsPT4* and *AsPT5* promoters upstream of the translation initiator, ATG, were amplified by iPCR using primers (Table S1) which contained *HindIII* and *BamHI* restriction sites at the 5' and 3' ends. After digestion with the two restriction enzymes, the amplified fragments were purified and cloned into the linearized binary vector, pBI121, to replace the CaMV35S promoter in front of the *GUS* gene (Chen *et al.*, 2011). The resulting constructs were the *AsPT1*, *AsPT4* and *AsPT5* promoter-*GUS* constructs. To investigate the possible involvement of the 5'UTR intron in the regulation of expression of *AsPT5*, two expression cassettes one without the intron (*pAsPT5-261::GUS*) and the other with the 5'UTR intron (*pAsPT5-1280::GUS*) were generated. The new vectors were transformed into *A. sinicus* roots by *A. rhizogenes*-mediated transformation (Li *et al.*, 2008).

Construction of the *AsPT4* promoter deletion series

A series of 5' truncations of the putative promoter sequence of *AsPT4* (670 bp) was created by PCR using specific primers (Table S1). The targeted deletion of the predicted MYCS sequence was generated by overlap and extension PCR (Table S1) for the promoter of *AsPT4*. The deletion and mutation promoter sequences were cloned into the *HindIII*- and *BamHI*-digested pBI121 binary vector to drive *GUS* gene expression. The resulting gene constructs were designated *AsPT4P-1* to *AsPT4P-5*.

Electrophoretic mobility shift assay

In order to examine the putative AM-specific responsive transcription factor binding sequences in promoter regions of *AsPT4*, the electrophoretic mobility shift assay (EMSA) was performed according to the published report (Frenzel *et al.*, 2006).

In situ hybridization

In situ hybridization was carried out as described previously (Kouchi & Hata, 1993; Liu *et al.*, 1998a,b; Daram *et al.*, 1999) using DIG-labelled antisense and sense probes synthesized from the 3' end cDNA of *AsPT1-4*. DIG-labelled probes were generated with the T7 or SP6 RNA polymerase (TaKaRa) from linearized pGM-T (Tiangen, Beijing, China) containing the corresponding cDNA. The probes were labelled with DIG following the procedure described by the manufacturer (Roche; Methods S1).

Subcellular localization of GFP fusion proteins in yeast and onion epidermal cells

The subcellular localization of *AsPT1* and *AsPT4* in yeast was performed with a C-terminal fusion of *AsPT1* or *AsPT4* to GFP in strain MB192 as described elsewhere (Reinders *et al.*, 2002). GFP was fused to the 3' ends of *AsPT1* and *AsPT4* (Wu *et al.*, 2011), then the fusion constructs CaMV35S-*AsPT1* and CaMV35S-*AsPT4* and the pBI-121-GFP empty vector were introduced into onion epidermal cells by a particle bombardment system (Biolistic PDS-1000/He System; Bio-Rad, USA) according to the manufacturer's instructions.

Complementation analysis of the *Pht1* genes in yeast

Complementation analysis was carried out as described previously (Daram *et al.*, 1999; Ai *et al.*, 2009). The full detailed procedure is given in Methods S1.

In order to determine the kinetic properties of the Pht1 transporters, Pi uptake experiments using ^{32}P i were performed with the positive yeast transformants. Approximately 1-mg (fresh yeast) cell samples were used following the previously described method (Ai *et al.*, 2009; Sun *et al.*, 2012).

Overexpression of *AsPT1* gene in mycorrhizal roots

The full-length ORF of *AsPT1* was cloned into the *KpnI* and *BamHI* sites of the plant expression vector pU1301. The resulting vector was called pU1301-*AsPT1*, and the *AsPT1* gene was driven by a maize ubiquitin promoter. The subclones were digested and sequenced to confirm their authenticity. Plant transformation was performed as described previously (Li *et al.*, 2008). The empty pU1301 vector was used as the negative control. The transgenic roots were selected using kanamycin (50 mg ml^{-1}) and the constitutive expression of GUS. First, the roots of Plantlets containing pU1301 vector are supposed to be kanamycin resistant. Second, we also did a GUS staining for each root by sampling their tips. We only chose the positively stained roots for further studies. The full detailed procedure is given in Methods S1.

Analysis of transgenic roots for the expression levels of the *AsPT1* transcript in *G. intraradices* symbiosis was performed as described previously (Dermatsev *et al.*, 2010).

AsPT1 and *AsPT4* RNAi constructs

Two independent *AsPT1* and *AsPT4* RNAi constructs were generated. For the *AsPT1* RNAi constructs, the regions corresponding to -120 to +99 and 1660 to 1931 nucleotides (relative to the ATG start codon) of *AsPT1* were amplified, using the primers *AsPT1*Ri5F containing *SpeI* and *KpnI* sites (5'-TA ACTAGTGGTACCGGGAGGGTTCCCCAAGTGC-3'), and *AsPT1*Ri5R containing *SacI* and *BamHI* sites (5'-TAGAGC TCGGATCCAGTGAAGAAACCCATACCAG C-3'); and *AsPT1*RiF2 containing *SpeI* and *KpnI* sites (5'-TAACTAGT GGTACCTGGAACCTTCAATAGTTTAG-3'), and *AsPT1*RiR2

containing *SacI* and *BamHI* sites (5'-TAGAGCTCGGATCCTGATGGTAGACTA CTAAGG-3'). The fragments were introduced into the pDS1301 vector (Chu *et al.*, 2006) at the *KpnI*-*BamHI* and *SacI*-*SpeI* sites to create the *AsPT1* RNAi-5' and *AsPT1* RNAi-3' constructs, respectively. Similar methods used for generating the *AsPT4* RNAi constructs are shown in Methods S1. All the RNAi constructs confirmed by restriction digestion and sequencing were transferred to *A. rhizogenes* strain K599 by electroporation, and were transformed into *A. sinicus* roots. The empty pDS1301 vector was used as the negative control.

Histochemical GUS assays and detection of fungal colonization

Histochemical GUS assays were performed as described previously (Chen *et al.*, 2010). Fresh transgenic roots were incubated in 1 mM X-gluc and 0.1% Triton X-100 (v/v) within 0.05 M sodium phosphate buffer (pH 7.0) at 37°C overnight. To visualize fungal structures, the stained material was counterstained at room temperature overnight with 0.01% acid fuchsin (Floss *et al.*, 2008). Stained material was analysed by microscopy (BX51, Olympus, Japan). Roots were stained with Trypan blue, and mycorrhizal colonization was examined and quantified using the program MYCOCALC according to the method described previously (Trouvelot, 1986).

For the investigation of arbuscule developmental stages, root fractions were stained at 25°C overnight with 0.01% acid fuchsin. The fungal structures within the roots were visualized by confocal laser scanning microscopy (LSM 510 Meta; Zeiss) using the 543 nm laser line for excitation. Arbuscule populations, arbuscule size and infection unit length were measured using Image J software (<http://rsb.info.nih.gov/ij/>) according to the method described by Zhang *et al.* (2010).

For enzymatic GUS assays, root tissues were ground in liquid nitrogen and transferred to microtubes containing the extraction buffer for total protein extraction (Chen *et al.*, 2010). Beta-glucuronidase activity was measured fluorimetrically using 1 µg of total protein extract, as described previously (Andriankaja *et al.*, 2007).

Histochemical vital and polyphosphate staining

Histochemical vital and polyphosphate stainings of AM fungus were performed as described previously (Schaffer & Peterson, 1993; Tatsuhiro & Sally, 2001; Ezawa *et al.*, 2004).

Estimation of total P content in plant tissue

Total P content was estimated using a phosphomolybdate colorimetric assay (Shin *et al.*, 2006).

In silico analysis of cloned genes

Analysis of the gene sequences was carried out utilizing the following programs: NCBI Blast Server for the homology searches (www.ncbi.nlm.nih.gov), ClustalW for multiple sequence alignment (www2.ebi.ac.uk/clustalw/) and PROSITE for detection of

conserved motifs (www.expasy.ch/prosite/). Hydropathy plots were analysed by TopPred (<http://www.sbc.su.se/~erikw/toppred2/>). Topology prediction programs SOSUI (<http://bp.nuap.nagoya-u.ac.jp/sosui/>) were used to predict the orientation of the transmembrane regions of Pht1 proteins. Phylogenetic tree analysis was performed using MEGA v4.1 phylogeny software (The Biodesign Institute, AZ, USA). Analyses of known *cis*-regulatory elements in the promoters were performed by searching the PLACE database (<http://www.dna.affrc.go.jp/htdocs/PLACE/>). Predicted conserved motifs were screened within the promoter regions of orthologous PiTs from diverse species using the FootPrinter v3.0 algorithm web server (<http://genome.cs.mcgill.ca/cgi-bin/FootPrinter3.0/FootPrinterInput2.pl>).

Statistical analyses

The data were analysed by ANOVA (SPSS 16.0; SPSS Inc., Chicago, IL, USA), followed by Turkey's HSD test ($P < 0.05$), to test differences between plant genotypes and treatments. The data represent the mean \pm SD of three independent replicates.

Results

Characterization of the novel mycorrhiza-specific *AsPT1* and *PHT1* transporters

Six putative *Pht1* genes were isolated from mycorrhizal *Astralegus sinicus* with degenerate primers, designated as *AsPT1* through *AsPT6* (Fig. 1). Among them, *AsPT1* (JQ956415), *AsPT3* (JQ956417) and *AsPT6* (JQ956420) contain no introns, whereas *AsPT2* (JQ956416) and *AsPT4* (JQ956418) have single introns, 196 and 699 bp in size, respectively. Interestingly, 5' end RACE showed that a large (965 bp) intron exists in the 5' untranslated region (UTR) of *AsPT5* (Fig. S1a). Southern blot analysis indicated that these Pi transporters of *A. sinicus* were single or low-copy genes (Fig. S1b). The deduced amino acid sequences of *AsPT1*-5 were aligned with the sequences of the Pht1 family from other plants (Fig. S2). Their multiple sequence alignment shows the five PiTs genes have the consensus sequence of 25 amino residue regions, LCFRRFWWLGFGIGGDYP LSA-TIMSE, including the Pht1 signature, GGDYPLSATIxSE (Karandashov & Bucher, 2005). However, the Pht1 signature was slightly modified in *AsPT1*; a Thr (T) was exchanged with a Val (V). All six predicted proteins are highly hydrophobic and contain 12 putative membrane-spanning regions with one big intracellular central loop (Fig. S3).

A phylogenetic tree further demonstrated that all of the Pi transporters cloned in this study are the orthologues of six members of the Pht1 family (Fig. 1). These Pht1 family genes can be roughly divided into four subfamilies with clade I (Pht1;1 and Pht1;4), clade II (Pht1;2), clade III (Pht1;3), and clade IV (Pht1;5 and Pht1;6). Interestingly, *A. sinicus* possesses at least two phylogenetically distant AM-associated Pht1 proteins.

The *cis*-elements analysis and phylogenetic footprinting revealed that the *cis*-regulatory element TAAT motif (TAATATAT) was present exclusively in the *AsPT1* and *AsPT4*. In the *AsPT1* and

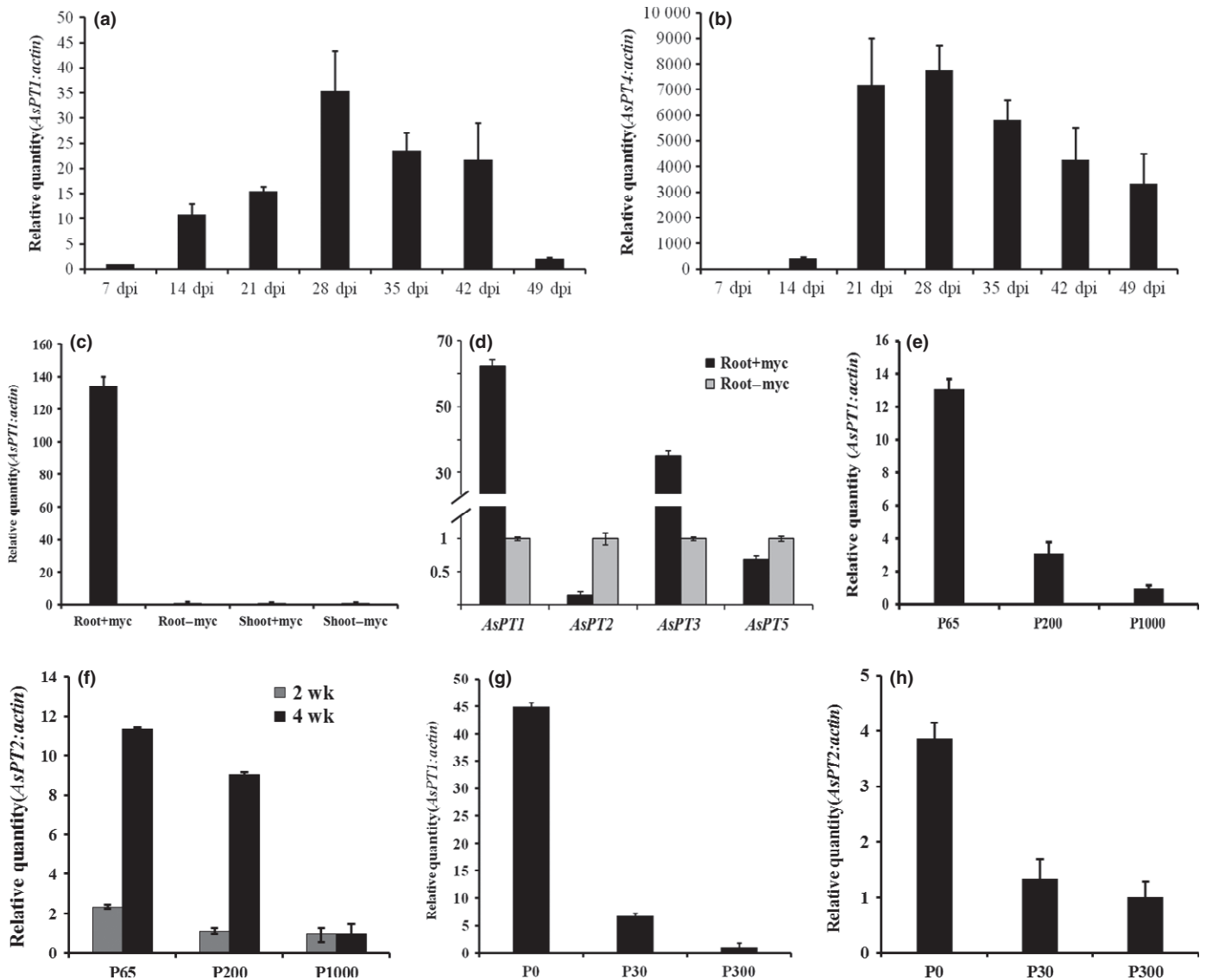


Fig. 2 Expression patterns of the Pht1 family genes in arbuscular mycorrhizal roots. (a) Real time RT-PCR analysis of *AsPT1* expression in mycorrhizal roots at 7, 14, 21, 28, 35, 42 and 49 d post-inoculation (dpi). The total colonization is 7.8%, 20.4%, 50.6%, 80.4%, 87.3%, 74.2% and 53.8%, respectively. (b) Real time RT-PCR analysis of *AsPT4* expression in mycorrhizal roots on the same samples as indicated in (a). (c) Real time RT-PCR analysis of the *AsPT1* expression in nonmycorrhizal and mycorrhizal roots or shoots (4 wk post inoculation (wpi)) grown under Pi starvation. (d) Expression levels for *AsPT1*, *AsPT2*, *AsPT3*, and *AsPT5* in nonmycorrhizal and mycorrhizal roots during phosphorus starvation. (e) Expression level of *AsPT1* in response to Pi availability. Total RNA was isolated from mycorrhizal roots (4 wpi) after treatment with 65, 200 and 1000 μM Pi, respectively, for 28 d. (f) mRNA levels of *AsPT2* in nonmycorrhizal roots at 14 d (grey bars) and 28 d (dark bars) after treatment with 65, 200 and 1000 μM Pi, respectively. (g) Expression of *AsPT1* in response to phosphate starvation in mycorrhizal transgenic roots (pBI121 vector) at 14 d after treatment with 0 μM (P0), 30 μM Pi (P30) and 300 μM Pi (P300). (h) mRNA levels of *AsPT2* in nonmycorrhizal transgenic roots at 14 d after treatment with 0 μM (P0), 30 μM Pi (P30) and 300 μM Pi (P300). *AsActin* was used as the internal standard. The means + SD of three independent determinations are presented.

65 μM was *c.* 11.5 times higher than that of 1000 μM Pi at 30 d after treatment (Fig. 2f).

In the *in vitro* system, the expression levels for *AsPT1* under Pi-starved conditions was enhanced 45-fold in the mycorrhizal transgenic roots (Fig. 2g). Similar to *AsPT1*, the expression of *AsPT2* and *AsPT3* was depressed by resupply of Pi in the transgenic roots (data not shown). Besides, the expression of *AsPT2* under Pi-starved conditions was enhanced 3.5-fold in the transgenic roots at 14 d after treatment (Fig. 2h).

Subcellular and tissue localization of Pht1 transporters

Plant Pht1 members were predicted to be localized to the plasma membrane. To investigate the subcellular localization of the *AsPT1* and *AsPT4* transporters, we constructed C-terminal protein fusions with GFP placed under the control of the strong 35S promoter. As expected, the two fused proteins were targeted to the plasma membrane (Fig. S6), confirming the potential transport activity of *AsPT1* and *AsPT4*.

For histochemical analysis, the promoters and 5' untranslated regions of *AsPT1* and *AsPT4* were fused to a GUS reporter gene. Subsequently, the constructs were transformed into *A. sinicus*. Four weeks after colonization, GUS activity

could be detected only in cells containing arbuscules (Fig. 3). To visualize AM fungal structures, the GUS stained material was counterstained with acid fuchsin staining (Fig. 3e,h).

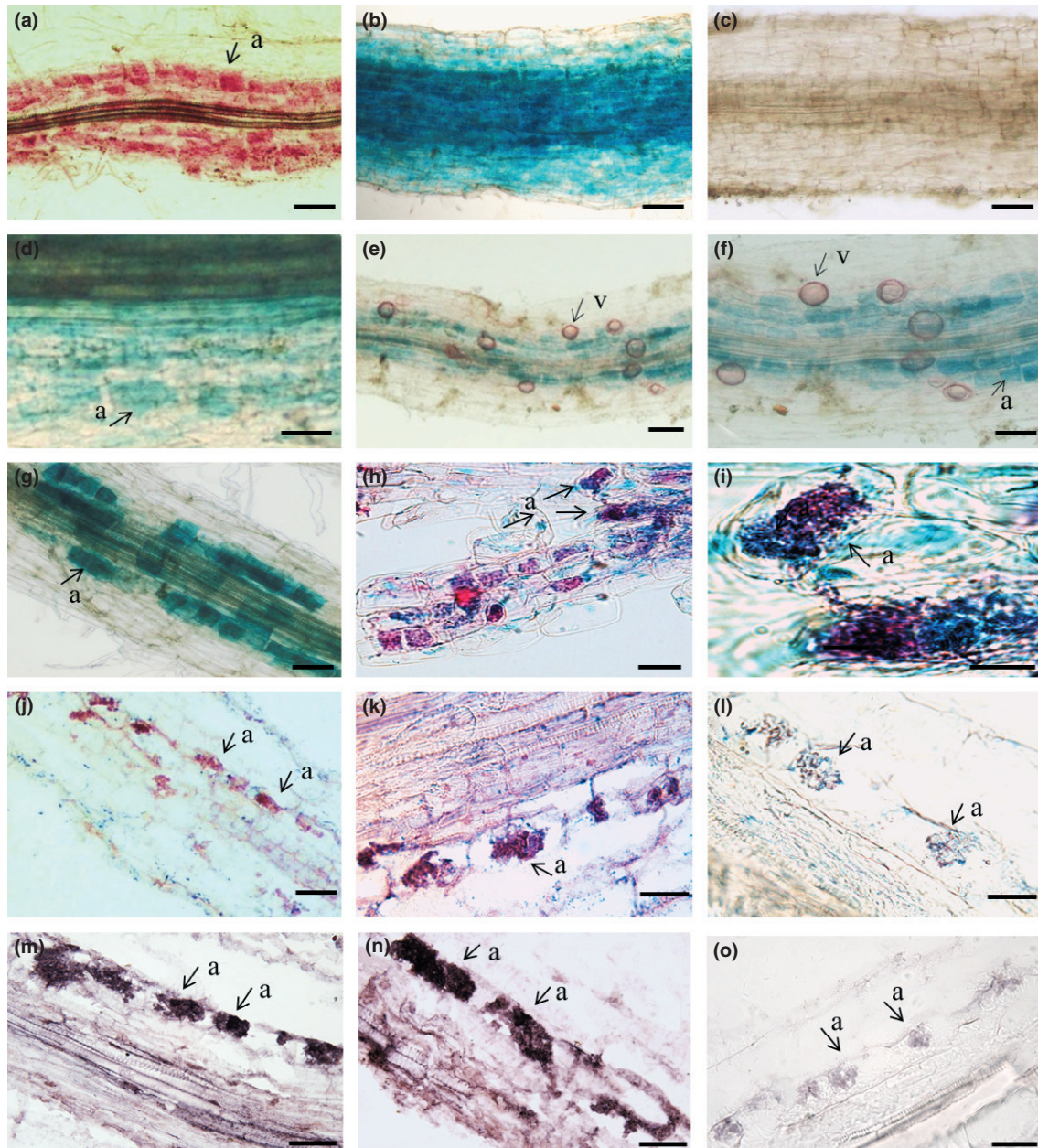


Fig. 3 Tissue localization of *AsPT1* and *AsPT4* in mycorrhizal *Astragalus sinicus* hairy roots. (a) to (i) *AsPT1* and *AsPT4* promoter activity in mycorrhizal *A. sinicus* hairy roots. (a) Negative control showing arbuscules in mycorrhizal roots transformed with the empty GUS vector (*pNOS: GUS*). (b) The positive control showing uncolonized roots with the promoter GUS constructs (*p35S: GUS*). (c) The control showing unmycorrhizal roots with the promoter GUS constructs (*pAsPT4: GUS*). (d–f) Activity of the *AsPT1* promoter in *A. sinicus* mycorrhizal roots. (d) Bright field image of roots colonized with *G. intraradices* reveal GUS expression in the cortical cells with arbuscules. (e) GUS stained material counterstained with acid fuchsin staining show arbuscules and vesicles. (f) Enlarged view of the arbuscules in (e). (g–i) Activity of the *AsPT4* promoter in *A. sinicus* mycorrhizal roots. (g) Roots colonized with *Glomus intraradices* reveal promoter activity in the inner cortical cells with arbuscule. (h) GUS stained material counterstained with acid fuchsin staining show arbuscules. (i) Enlarged view of the arbuscules in (h). a, arbuscules; v, vesicles. Bars, 25 μ m. (j–o) *In situ* localization of the *AsPT1* and *AsPT4* transcripts in arbuscule mycorrhizal roots of *A. sinicus*. (j, k) Longitudinal sections (8 μ m) from *A. sinicus* roots colonized by *G. intraradices* and probed with DIG-labelled RNA probes for *AsPT1*. (l) Sections probed with sense probes as negative controls. (m, n) Longitudinal sections from AM roots were probed with antisense RNA probes for *AsPT4*. (o) Sections were probed with DIG-labelled sense probes as a negative control. *In situ* hybridizations were repeated at least three times with equivalent results. a, arbuscules. Bar, 100 μ m.

In order to confirm the correlation between the *AsPT1* and *AsPT4* expression pattern observed by q RT-PCR and GUS staining, we examined the accumulation of *AsPT1* and *AsPT4* mRNA in mycorrhizal *A. sinicus* using *in situ* hybridization. These results revealed that the *AsPT1* and *AsPT4* transcripts were restricted to the arbusculated inner cortical cells (Fig. 3j,m). The patterns of labelled signals were in agreement with the PCR and reporter gene expression patterns described above. In addition, *AsPT2* transcript was detectable in the root tip and epidermis under Pi-starved conditions (Fig. S7). *AsPT3* was localized in root sectors where mycorrhizal structures are formed, and in the cortex cells and epidermis (Fig. S7k). In transgenic plants carrying *AsPT5* promoter without intron, the GUS activity was present exclusively in the central cylinder of hairy roots (Fig. S7p). However, lines carrying *AsPT5* promoter with intron, GUS expression was present in the central cylinder and root tips (Fig. S7q,r).

Functional *cis*-elements mediate AM-activated *AsPT4* gene expression

In order to identify the putative *cis*-elements located within the putative promoter regions that are required for mycorrhiza-specific *AsPT4* gene expression, a series of expression cassettes with truncated promoter fragments and a GUS reporter gene were generated (Fig. 4a), and then introduced into *A. sinicus* roots. The transgenic plants were subsequently inoculated with *G. intraradices* and analysed. A significant decrease in the level of GUS expression was observed following the deletion of *Pht1;4* promoter up to -226 bp as compared to that of the full-length promoter, even though the mycorrhization rate was not significantly different (Fig. 4b). The two motifs (TAAT and TAAC) located within this region might mediate AM-activated expression of *AsPT4*. However, further truncation of the promoter to -194 , which includes the first P1BS motif, slight GUS activity reduction was observed. Deletion of *pAsPT4* down to -161 (*AsPT4p-4*), resulted in a decrease of GUS activity (Fig. 4a,b). This finding suggests that the P1BS motif is necessary for the AM-inducible activation. Further deletion up to -129 , which includes the MYCS and TGTT motifs, led to lower GUS activity in the roots.

In order to determine whether MYCS is essential for the AM-activated expression of *AsPT4*, we generated a construct (*AsPT4p-M*) with knockout of this motif (TTTCTTGTTTC) from the truncation *AsPT4p-2*. As observed, the deletion of MYCS resulted in a strong decrease of GUS activity in the transgenic lines (Fig. 4c). The data highlight that MYCS is a functional *cis*-element mediating AM-activated *AsPT4* gene expression.

In order to specify the binding sites of the AM-specific responsive *cis*-elements, the putative protein binding sites of the *AsPT4* promoter were analysed by EMSA. The fragments for DNA-protein binding assays are the putative motifs: MYCS, TGTT, TAAC and TAAT. These four fragments showed a gel shift after incubation with protein extract from mycorrhizal roots (Fig. 4d). Remarkably, no shifts occurred in the control experiments. It means corresponding promoter fragments are only recognized and bound by protein factors in mycorrhizal roots.

Functional analysis of the *AsPT1* and *Pht1* family in yeast

In order to obtain the biochemical evidence for the function of the *Pht1* family, yeast mutant MB192 was used for complementation analysis. The *AsPT1* and *AsPT5* functionally complemented the mutant (Fig. 5a,b). By contrast, yeast cells expressing *AsPT2*, *AsPT3* and *AsPT4* were not able to grow on low-Pi medium. In addition, GFP-*AsPT1* or GFP-*AsPT4* fusions were introduced into the mutant MB192. In agreement with the localization observed in plant cells (Fig. S6), the GFP signal was clearly detected at the periphery of the yeast cell (Fig. 5c), indicating that the full-length *AsPT1* and *AsPT4* proteins are targeted to the yeast plasma membrane, which is a prerequisite for transporting phosphate.

The pH dependence of Pi transport by *AsPT1* was measured over a range of pH values. Growth of the MB192 yeast strain expressing *AsPT1* was optimal on acidic pH medium, with a sharp pH optimum at 4.5 (Fig. 5e).

In order to determine the kinetic properties of *AsPht1* family, Pi uptake experiments using ^{32}Pi were performed in the transformed yeast mutant. Uptake rates of ^{32}Pi at different Pi concentrations showed that Pi uptake mediated by *AsPT1* followed Michaelis–Menten kinetics, exhibiting an apparent mean K_m of 31.12 ± 5.87 μM Pi (Fig. 5f). These results indicate that *AsPT1* is a high-affinity Pi transporter. We next monitored direct Pi uptake of other *Pht1* family transporters, the apparent K_m values ranged from 46.75 ± 19.54 μM for *AsPT5* (Fig. S8) to 128.7 ± 60.17 μM for *AsPT3* (data not shown), showing that the *AsPT5* transporter is able to mediate high-affinity Pi acquisition as well.

AM symbiosis in *A. sinicus* showing development promotion by overexpression of *AsPT1*

In order to characterize the role of *AsPT1* in the development of AM symbiosis in planta, an *AsPT1* overexpression assay was performed. Overexpression efficiency of *AsPT1* in roots was confirmed by qRT-PCR analyses. Under the Pi-deficient condition, the *AsPT1*-OE roots showed enhanced amounts of the transcript compared with the controls (Fig. 6f). A hastening growth of 42-d-old *AsPT1*-OE AM roots under LP (30 μM) supply was observed (Fig. 6b). The total amount of Pi accumulated in the transgenic roots was increased by *AsPT1*-OE (Fig. 6c). Relative to the controls, *AsPT1*-OE roots showed an increased density of mycorrhizal structures and abundance of arbuscules (Fig. 6d). Moreover, the majority of arbuscules in *AsPT1*-OE roots were significantly larger and more mature (Fig. 6a). However, no significant difference in the total colonization was found between control and *AsPT1*-OE roots. Hence, *AsPT1* is able to maintain development of the AM symbiosis in *A. sinicus*.

In addition, overexpression of *AsPT1* also affected expression of other *Pht1* members in *A. sinicus*. The expression levels of *AsPT2* and *AsPT5* were elevated in mycorrhizal *AsPT1*-OE transgenic roots, whereas the *AsPT6* gene was downregulated upon overexpression of *AsPT1* (Fig. 6g).

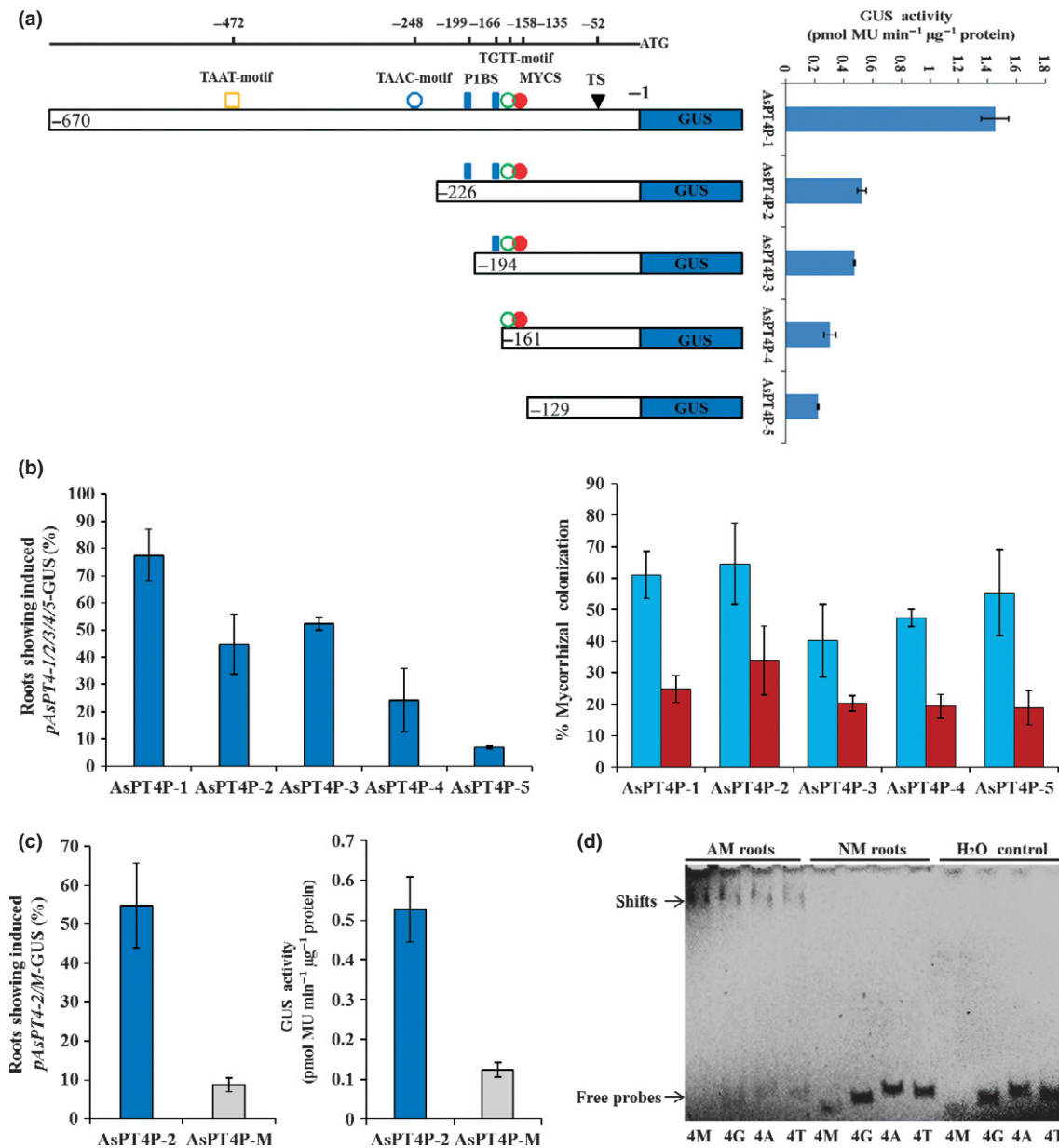


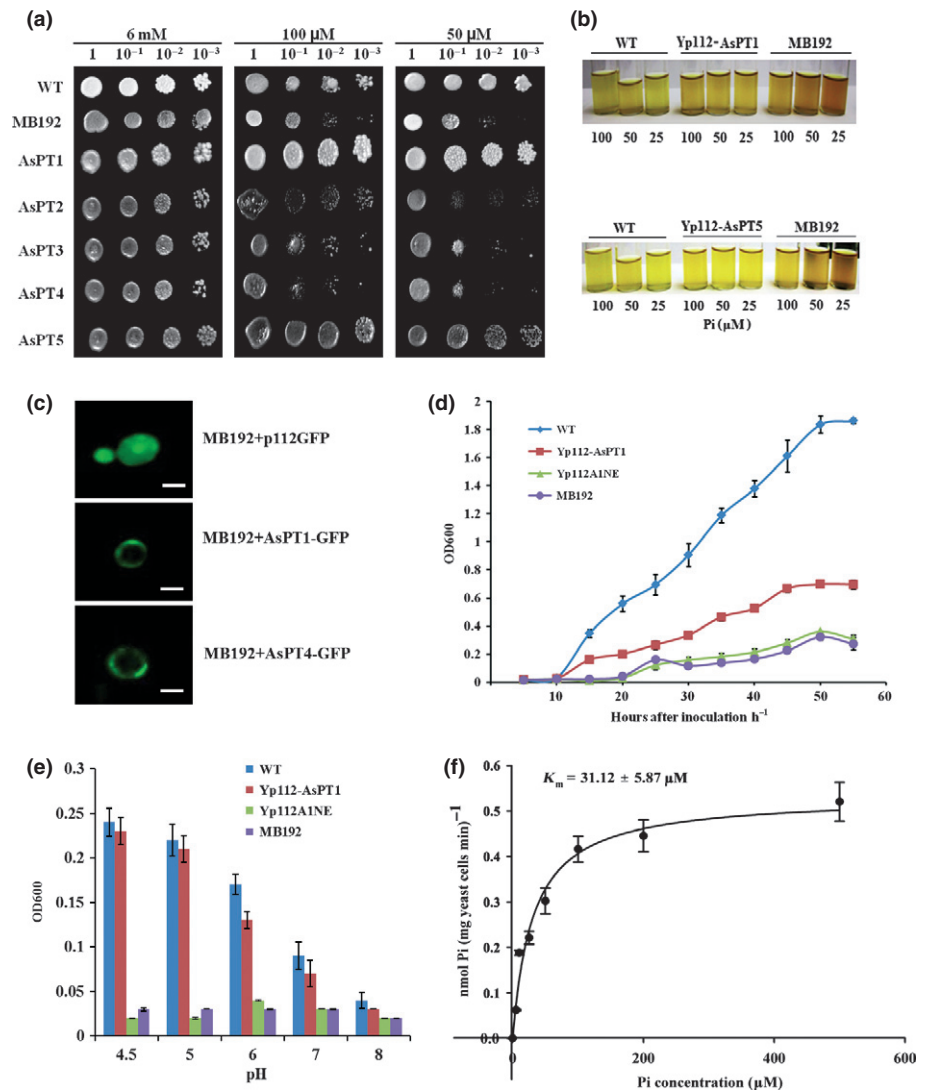
Fig. 4 Functional analyses of the conserved *cis*-elements involved in mycorrhiza-regulated activation. (a) Diagram of *AsPht1;4* promoter and deletion derivatives. Numbers inside the bars indicated the end point position of each deletion. Negative number 1 (–1) represents the first nucleotide on the 5' side of the translation start codon. The positions of the putative AM-specific responsive elements (symbols) in promoter regions of mycorrhiza-specific *AsPT4* are indicated. The relative strength of GUS activity in mycorrhizal roots driven by the chimeric promoters with various truncated versions of the promoter. The GUS activity in protein extracts from individual roots was measured quantitatively using fluorimetric assays. Error bars indicate \pm SD. (b) The relative strength of GUS activity is presented as the percentage of various truncated mycorrhizal roots exhibiting induced GUS activity. Percentage of hairy roots colonized by total fungal structures (F, light blue bars) and arbuscules (A, red bars) of *Glomus intraradices* in various truncated lines as indicated at 4 wk post-inoculation (wpi). Mean values of three biological replicates are shown. (c) The relative strength of GUS activity is presented as the percentage of mycorrhizal roots exhibiting induced GUS activity. The GUS activity driven by truncated versions *AsPT4P-2* and *AsPT4P-M* of *AsPT4* promoter. *AsPT4P-M* indicates the MYCS deletion mutation in *AsPT4P-2*. (d) Electrophoretic mobility shift assay of *AsPT4* promoter. EMSA was carried out with protein extract from mycorrhizal or nonmycorrhizal roots and without proteins (control). Positions of the analysed promoter fragments are the putative mycorrhiza-specific motifs: 4M(51 bp), 4G(58 bp), 4A(64 bp) and 4T(61 bp) indicate that these fragments contain MYCS, TGTG, TAAC, and TAAT motifs, respectively.

AsPT1 and *AsPT4* are indispensable for AM development in *A. sinicus*

In order to further examine the function of *AsPT1* and *AsPT4* in AM symbiosis, *AsPT1* and *AsPT4* RNAi constructs were

generated, to investigate their effects on the development of the AM symbiosis. Knockdown efficiency of *AsPT1* and *AsPT4* was confirmed by qRT-PCR analyses. In AM roots, the transcript levels of *AsPT1* in the RNAi lines were *c.* 6% and 23% of the controls, respectively (Fig. 7a). Similarly, *AsPT4* was effectively

Fig. 5 Functional characterization of Pht1 family in the yeast mutant strain MB192. (a) Yeast MB192 cells harbouring either an empty expression vector p112A1NE (control) or the full-length cDNAs of *AsPT1*, *AsPT2*, *AsPT3*, *AsPT4*, or *AsPT5* constructs were grown in SD medium at pH 5.8 to an $OD_{600} = 1$. Equal volumes of 10-fold serial dilutions were plated on plates containing 6 mM Pi, 100 μ M Pi or 50 μ M Pi then incubated at 30°C for 3 d. (b) Staining test for acid phosphatase activity in the yeast strain MB192 (control); Yp112-*AsPT1*, which contains *AsPT1* in MB192; Yp112-*AsPT5*, which contains *AsPT5* in MB192; and the wild-type (WT). The YNB medium contained 25, 50 and 100 μ M Pi, respectively. (c) Fluorescence microscopy images of yeast cells harbouring either the vector p112GFP, the p112GFP-*AsPT1*, or the p112GFP-*AsPT4* plasmid after induction of recombinant protein production. Bar, 25 μ m. (d) Growth curves of the wild-type, MB192 and MB192 transformed with Yp112-*AsPT1* generated from a 55-h culture under 25 mM MES buffer and 50 μ M Pi. (e) The effect of pH on the growth of the four yeast strains: WT, Yp112-*AsPT1*, Yp112 and MB192. OD_{600} values showed means \pm SD for three replicates, and the medium contained 50 μ M Pi and 25 mM MES buffer. (f) Michaelis–Menten kinetics of 32 Pi uptake. The nonlinear regression of Pi uptake of strain Yp112-*AsPT1* vs external Pi concentration at pH 4.5 was used to estimate the apparent K_m value for Pi uptake.



silenced in AM roots (Fig. 7b). Relative to the controls, *AsPT1* RNAi roots showed a reduced extent of arbuscule formation and overall fungal colonization (Fig. 8b). Similarly, total colonization and arbuscules rate were significantly reduced also in *AsPT4* RNAi roots (Fig. 8c). Hence, *AsPT1* and *AsPT4* are indispensable but not functionally redundant for normal development of the AM symbiosis in *A. sinicus*.

In order to examine the symbiotic phenotype at the molecular level, we analysed the expression of other *Pht1* members in *AsPT1* or *AsPT4* RNAi lines. Interestingly, the *AsPT4* mRNA levels in the *AsPT1* RNAi lines remained as high as in the controls (Fig. 7c), despite the reduced total colonization and arbuscule formation, indicating compensatory effects between the two transporters. Transcript levels of *AsPT1* in *AsPT4* RNAi lines were significantly reduced relative to the controls (Fig. 7d). *AsPT2* was also downregulated upon suppression of *AsPT1* or *AsPT4*; however, *AsPT3* showed unaltered transcript levels in all the RNAi lines. In *AsPT1* RNAi lines, no reduction of *AsPT5* mRNA was observed, by contrast, *AsPT5* mRNA in *AsPT4* RNAi lines was reduced relative to the controls. Transcript levels of

AsPT6 were upregulated in the *AsPT1* and *AsPT4* RNAi roots (Fig. 7c,d).

Knockdown of *AsPT1* or *AsPT4* by RNAi results in a premature death of the arbuscule phenotype

AsPT1 and *AsPT4* RNAi lines were analysed to determine the morphology of arbuscule. Transgenic roots expressing RNAi construct designed to target *AsPT4* showed a mycorrhizal phenotype identical to that of *AsPT1* RNAi lines. The fungus was able to penetrate the roots, but arbuscule development was impaired, degenerating and premature death arbuscules were visible in the cortical cells (Fig. 8a). To evaluate the proportion of the various stages of arbuscule development, three stages of arbuscule development and decay were defined. As deduced from a total of *c.* 900 evaluated arbuscules, a shift towards degenerating and dead arbuscules at the expense of mature ones occurred in *AsPT1* or *AsPT4* RNAi roots relative to the controls (Fig. 8d). Furthermore, lengths of arbuscules and infection units in *AsPT1* RNAi lines were significantly shorter than those in the controls

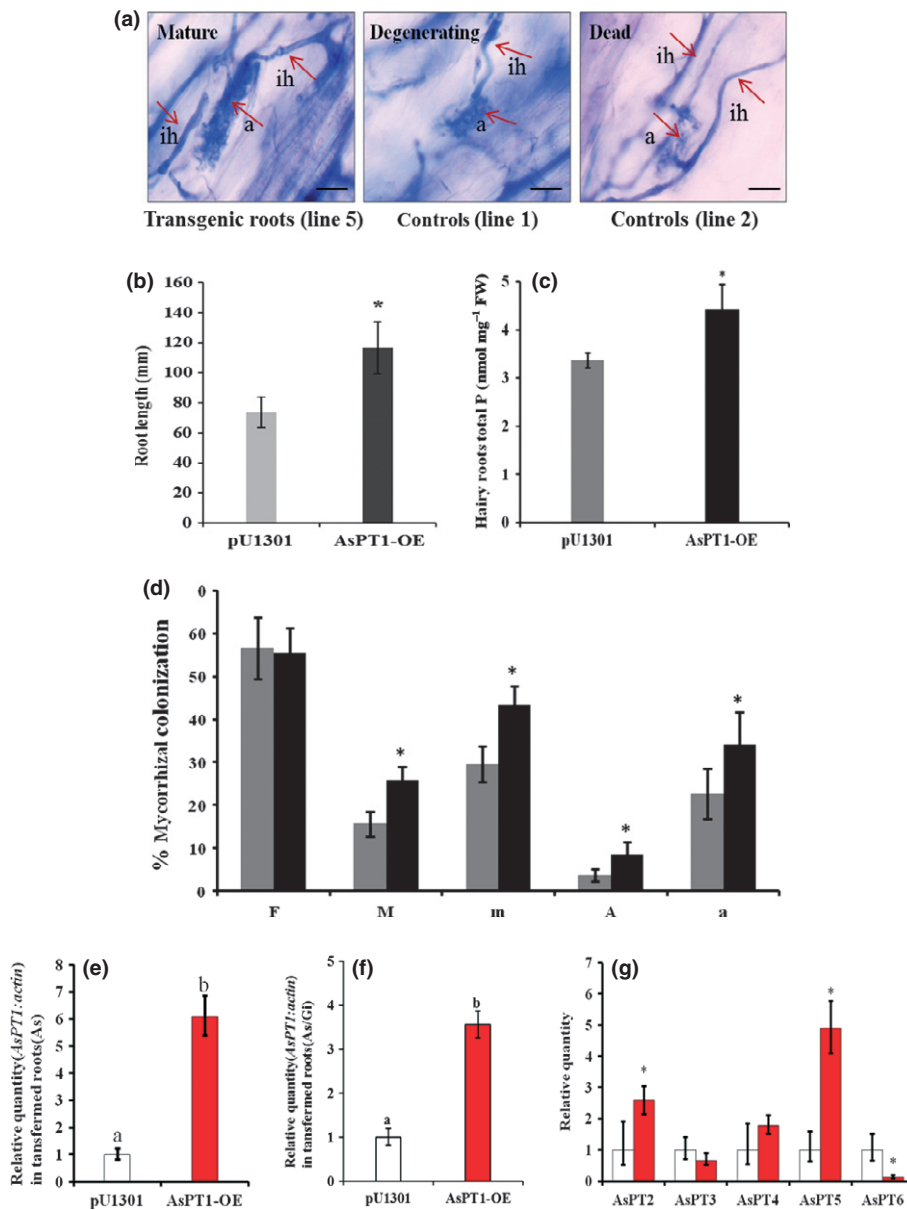


Fig. 6 Arbuscular mycorrhizal (AM) phenotypes of *AsPT1* transgenic roots. (a) Microscopy images of transgenic roots expressing an *AsPT1*-OE (overexpression) or control constructs colonized with *Glomus intraradices*. lh, internal hyphae; a, arbuscules. Bars, 100 μ m. (b) Mean root lengths of *AsPT1*-OE lines and roots transformed with empty pU1301 vector (control) after 42 d post-inoculation (dpi) with *G. intraradices*. (c) Hairy root P content of the transgenic plants at 42 dpi with *G. intraradices*. (d) Estimations of mycorrhization levels in *AsPT1*-OE hairy roots in comparison with control roots at 42 dpi. The parameters measured are frequency (F%) and intensity of mycorrhiza (M%) and arbuscule (A%) abundance; intensity in mycorrhizal root fragments (m%), arbuscule abundance in mycorrhizal root fragments (a%). Asterisks indicate a significant difference from *AsPT1*-OE lines ($P < 0.05$). (e–g) Molecular phenotypes of *Astragalus sinicus* *AsPT1*-OE transgenic roots. (e) *AsPT1* transcript accumulation in nonmycorrhizal *AsPT1*-OE and control roots. (f) *AsPT1* transcript accumulation in mycorrhizal *AsPT1*-OE and control roots. (g) Expression of five members of *A. sinicus* Pht1 family in the control and *AsPT1*-OE transgenic roots colonized with *G. intraradices*. White bars, control roots; red bars, *AsPT1*-OE roots. Different letters indicate samples that differ significantly from each other ($P < 0.05$). Error bars indicate \pm SD.

(Fig. 8e). Septate hyphae were observed in small arbuscules (Fig. 8a), indicating arbuscule collapse and death in *AsPT1* or *AsPT4* RNAi roots. The vital staining revealed that the incidences of live arbuscules were low in *AsPT1* or *AsPT4* RNAi roots (Fig. 8f). Thus, *AsPT1* and *AsPT4* are not only indispensable for intraradical fungal development, but also essential for arbuscule development in AM symbiosis.

AsPT4 but not *AsPT1* is required for Pi transfer in AM symbiosis

In order to evaluate the contribution of *AsPT1* and *AsPT4* to symbiotic Pi uptake, Pi uptake measurements were performed. Pi concentration was determined in shoot tissue of *AsPT1* and *AsPT4* RNAi lines when grown under low Pi supply in the presence or absence of *G. intraradices*. The shoot Pi content and shoot mass of NM plants were similar in all transgenic lines,

indicating that silence of *AsPT1* or *AsPT4* function had no effect on Pi nutrition in the absence of symbiosis (Fig. 9a,b). However, a significant increase in shoot Pi concentrations and shoot mass associated with *G. intraradices* treatment was apparent in the controls (Fig. 9). As observed in *M. truncatula* *PT4* mutants (Javot *et al.*, 2007a), *AsPT4* RNAi plants inoculated with *G. intraradices* did not differ significantly from NM plants, suggesting that *AsPT4* is essential for the symbiotic Pi uptake. By contrast, the *AsPT1* RNAi plants displayed Pi concentration in colonized plants as high as in the controls (Fig. 9a).

As an alternative, we used polyP staining to confirm whether loss of *AsPT1* or *AsPT4* function affected the symbiotic Pi transfer in the AM roots. The polyP granules accumulated in intraradical fungal vesicles and arbuscules within the *AsPT4* RNAi roots but not in wild-type, vector controls or *AsPT1* RNAi lines (Figs 9c, S9). The polyP staining patterns are consistent with the shoot P data (Fig. 9a,b) and suggest that loss of *AsPT4* function

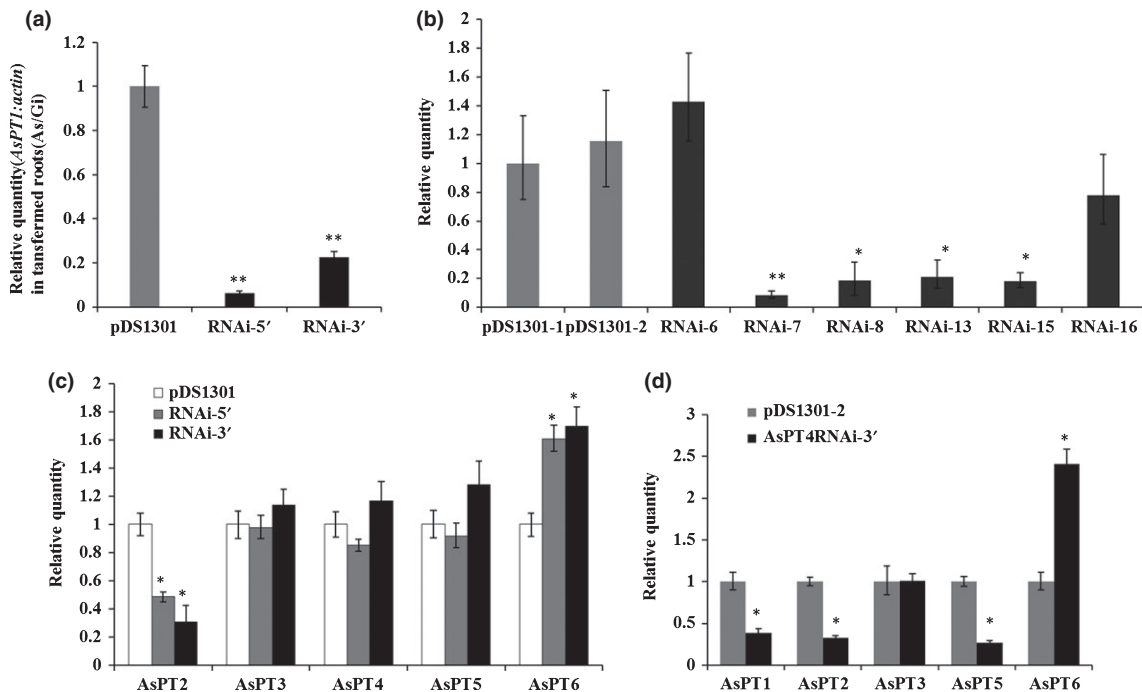


Fig. 7 Molecular phenotypes of the *AsPT1*RNAi and *AsPT4*RNAi roots. (a) Real-time quantitative RT-PCR analysis of *AsPT1* RNAi transgenic roots at 28 d post-inoculation (dpi). (b) Real-time PCR analysis of *AsPT4* RNAi roots at 28 dpi. Grey bars represent roots transformed with the empty pDS1301 vector as a control, and black bars represent roots transformed with the *AsPT1*RNAi construct. Transcripts are expressed as a ratio relative to β -actin transcripts in mycorrhizal roots. (c) Expression of five members of the *Astragalus sinicus* Pht1 family in the empty pDS1301 vector control and *AsPT1* RNAi plants with *G. intradices* under low P conditions (65 μ M Pi). White bars represent the vector controls, grey bars represent *AsPT1* RNAi-5' and black bars represent *AsPT1* RNAi-3' roots. (d) Expression of five members of *A. sinicus* Pht1 family in the vector controls and *AsPT4* RNAi roots. Grey bars represent the vector controls, and black bars represent *AsPT4* RNAi-3' UTR roots. Asterisks indicate lines that differ significantly from each other ($P < 0.05$). Error bars represent \pm SD for three independent transformants per line and three technical replicates.

results in a block in symbiotic Pi transfer from the fungus to the plant. In summary, these results showed that *AsPT4* is required for symbiotic Pi transfer in AM symbiosis and *AsPT1* do not compensate for the loss of *AsPT4*.

Discussion

AsPT4 paralogue *AsPT1* is a novel AM-specific Pht1 phosphate transporter

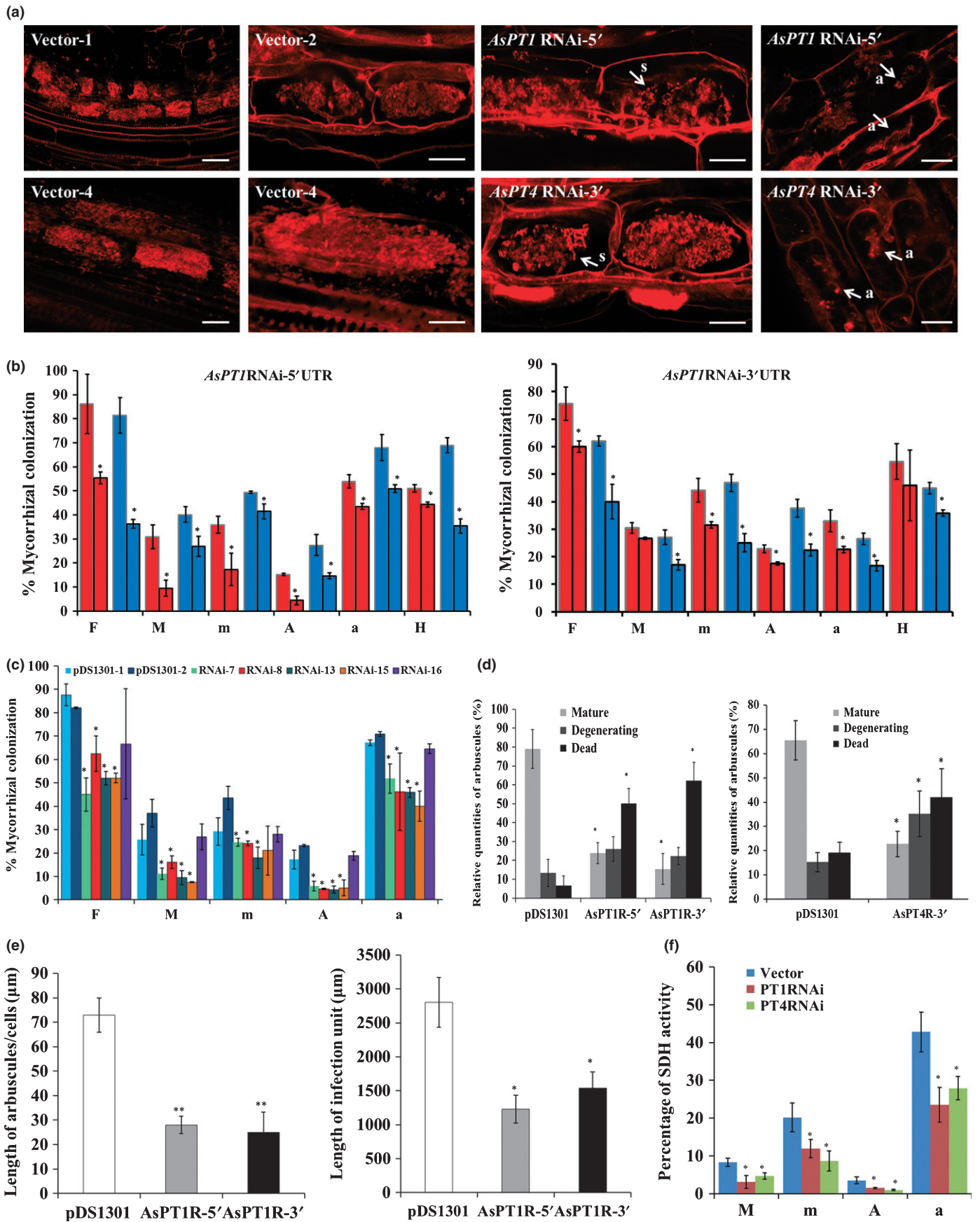
MtPT4, OsPT11 and StPT4 probably derived from the same ancient ancestor protein that existed long before the divergence of monocot and dicot lineages. MtPT4 orthologue *AsPT4* is an AM-specific Pi transporter with expression in the presence of symbiosis, supporting the evolutionary conservation of proteins involved in symbiotic Pi transport. Evolutionarily more recent, the legume species obtained an additional mycorrhiza-specific Pi transporter, *AsPT1*, which is phylogenetically distant from *AsPT4*. This finding indicates that *AsPT1* should play a different role in AM symbiosis. In addition, the *AsPT1* homologues in di- and monocotyledons currently form a novel gene subfamily attribute to gene duplication. *GmPT7* from *Glycine max*, for instance, is induced in the later stages of symbiosis (Tamura *et al.*, 2012); and the homologous *PrPT8* is phylogenetically associated to the AM-inducible Pht1 subfamily (Loth-Pereda *et al.*, 2011). Indeed, *BdPT12* and *BdPT13* are induced

during AM symbiosis (Hong *et al.*, 2012), similar to *OsPT13* (Yang *et al.*, 2012).

Functional diversity of the Pht1 family in arbuscular mycorrhizal *Astragalus sinicus*

Spatial expression patterns for the Pht1 family were performed by cellular localization analysis. The *AsPT1* and *AsPT4* were detected exclusively in arbuscule-containing cells of the cortex (Fig. 3). The *AsPT2* transcript is localized to the root tip and epidermis during Pi starvation (Fig. S7). The expression pattern is similar to *LePT1* and *LePT2* (Liu *et al.*, 1998b; Bucher *et al.*, 2001), suggesting that the *AsPT2* transporter plays a significant role in phosphate acquisition at the root–soil interface from soil. *AsPT3* occurred in mycorrhizal roots and root cortex cells. *AsPT5* sharing similarity with *OsPT2* (Ai *et al.*, 2009), is expressed in the central cylinder and root tip (Fig. S7). It is reasonable to conclude that *AsPT5* probably functions in the transport of Pi from roots to shoots. Thus, the distinct expression patterns of the *Pht1* members of *A. sinicus* in response to the arbuscular mycorrhizas, Pi starvation, and tissues indicated functional diversification.

Pht1 proteins share similarity with the proton-coupled Pi symporters from yeast and the mycorrhizal fungi (Fig. 1). Apparent K_m values of Pht1 transporters for Pi have been calculated from many such proteins via their expression in yeast mutants (Rausch *et al.*, 2001; Harrison *et al.*, 2002; Ai *et al.*, 2009; Jia *et al.*, 2011;



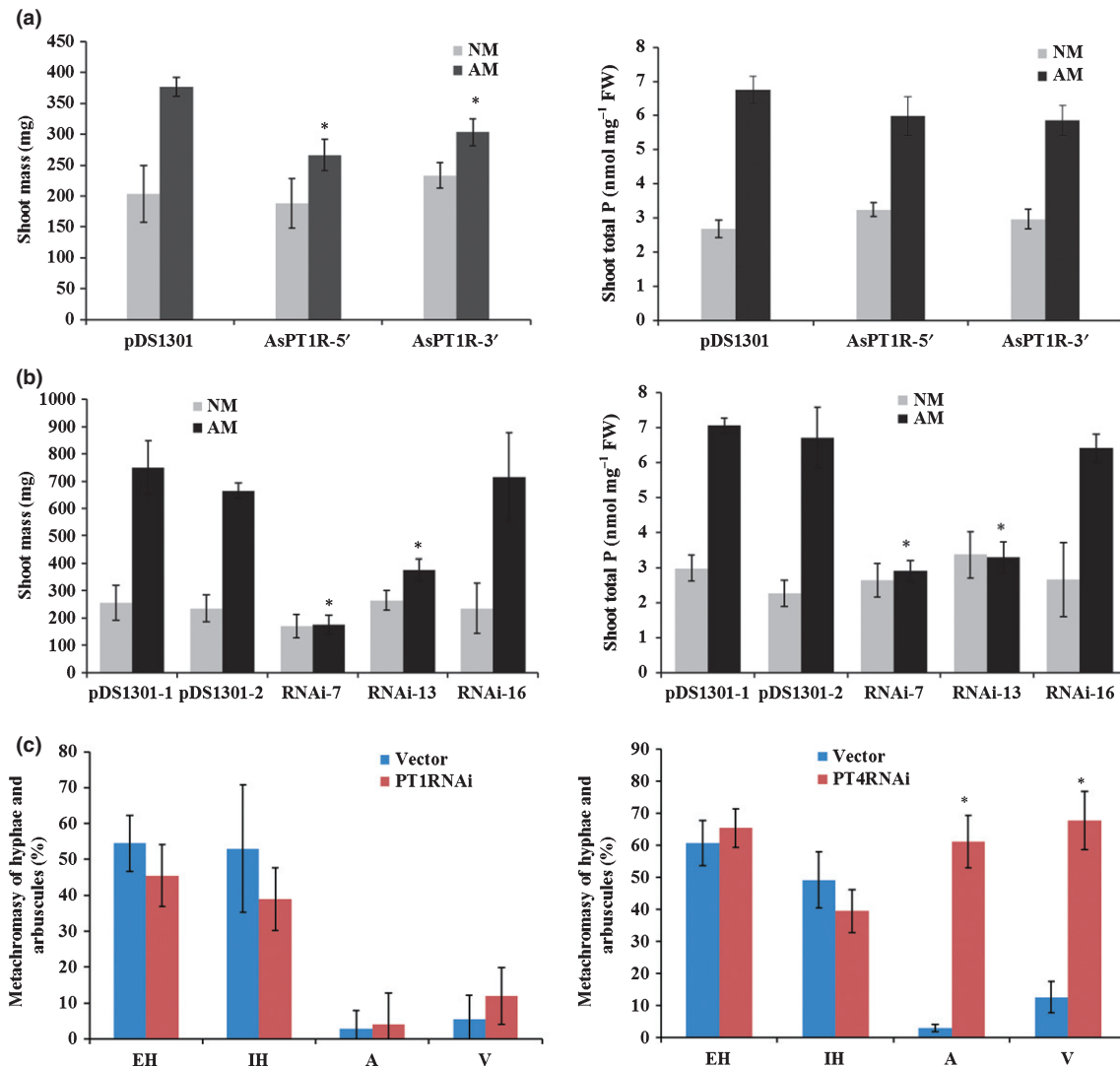


Fig. 9 Physiological analyses of the *AsPT1* RNAi and *AsPT4* RNAi transgenic plants. (a) Shoot mass and shoot P content of the *AsPT1* RNAi plants at 28 d post-inoculation (dpi) with *Glomus intraradices* (black bars) or the vector controls (grey bars). (b) Shoot mass and shoot P content of the *AsPT4* RNAi plants at 28 dpi with *G. intraradices* (black bars) or the vector controls (grey bars). (c) Assessment of polyphosphate in extraradical hyphae, intraradical hyphae, arbuscules and vesicles of *G. intraradices* in the pDS1301 and *AsPT1* or *AsPT4* RNAi roots by Toluidine blue O staining. Polyphosphate was localized by metachromasy of Toluidine blue O and the percentage of hyphae and arbuscules with metachromatic granules was assessed at 28 dpi. The mean SD of 100 intersections (the biological replicates of roots for each construct = 3) are presented. Asterisks indicate significant differences from pDS1301 at $P < 0.05$.

Remy *et al.*, 2012). Complementation of the yeast *Δpho84* mutant's growth defect at micromolar Pi concentrations, supported by a Pi uptake assay, demonstrates that *A. sinicus* Pht1;5

protein is indeed capable of mediating high-affinity Pi transport. The apparent K_m value for Pi uptake of 46.75 μM determined here for Pht1;5. The K_m values calculated for mycorrhiza-specific

Fig. 8 Arbuscular mycorrhizal (AM) phenotypes of *AsPT1* RNAi and *AsPT4* RNAi roots. (a) Confocal laser scanning electron microscopy images showing arbuscules in transgenic roots expressing the pDS1301 empty vector, *AsPT1* RNAi-5' or *AsPT4* RNAi-3' UTR constructs. Roots were stained with acid fuchsin. Arbuscules in control roots are large with many full hyphal branches; however, the collapsed hyphal masses contain many septa (arrows) in RNAi lines. a, arbuscules; s, septa. Bars, 20 μm. (b, f) AM phenotypes of the *AsPT1* RNAi and *AsPT4* RNAi transgenic plants. (b) Mycorrhization parameters in the empty pDS1301 vector control and *AsPT1* RNAi plants. Red and blue bars indicate acid fuchsin staining and trypan blue staining, respectively; grey and black border indicate control and *AsPT1* RNAi roots, respectively. (c) Estimations of mycorrhization levels in *AsPT4* RNAi hairy roots in comparison with control roots at 28 d post-inoculation (dpi). The parameters measured are frequency (F%) and intensity (M%) of mycorrhiza and arbuscule (A%) abundance; intensity in mycorrhizal root fragments (m%), arbuscule abundance in mycorrhizal root fragments (a%). Asterisks indicate a significant difference from *AsPT4* RNAi lines ($P < 0.05$). (d) Proportion of three different developmental stages among the total population of arbuscules classified after staining with acid-fuchsin. Approximately 100 arbuscules from each sample were evaluated. (e) Length of *Glomus intraradices* arbuscules in *AsPT1* RNAi roots, and empty vector. Lengths of infection units in roots transformed with the empty pDS1301 vector are significantly longer than those in *AsPT1* RNAi roots at 28 dpi. Asterisks indicate a significant difference ($P < 0.05$). Error bars represent ± SD. (f) Vital staining of controls and *AsPT1* or *AsPT4* RNAi roots colonized with *G. intraradices*. Vital staining reveals living fungal structures (hyphae and arbuscules). Asterisks indicate significant differences from pDS1301 at $P < 0.05$.

Pi transporters were 64 μM of StPT3 (Rausch *et al.*, 2001) and 493/668 μM for MtPT4 using two different yeast mutants (Harrison *et al.*, 2002), respectively. Importantly, our detailed functional analysis of AsPT1 and AsPT4 in yeast, indicated that AsPT1 encoded a functional high-affinity transporter, whereas AsPT4 as its orthologue MtPT4 was a low-affinity transporter. According to a previous hypothesis (Nagy *et al.*, 2005), the periferungal Pi concentration in roots can vary substantially, probably depending on the physiology of the symbiotic fungus. The coordinated activity of the symbiotic Pi transporters would ensure efficient uptake of fungal Pi (Smith *et al.*, 2003). In addition, the differences between complementation results and uptake measurements are due to the Δpho84 mutant that possesses other high- or low-affinity Pi transporters.

AsPT1 and AsPT4 are required for AM symbiosis

It is interesting that dicot species have at least two AMF-inducible phosphate transporter genes clustering separately with two Pht1 subfamilies. Knock out of *LePT4* in tomato indicated a high degree of functional redundancy between the two mycorrhiza-specific phosphate transporters, *LePT4* and *LePT5* (Nagy *et al.*, 2005). It would be useful to know whether the *AsPT1* and *AsPT4* also have a similar genetic redundancy of a Pi transporter as observed in tomato. If not, the distinct functions between AsPT1 and AsPT4 represent a novel subfamily of AM-specific PHT1 proteins in plants. A detailed phenotypic analysis revealed that *AsPT1* or *AsPT4* is indispensable for the formation of AM symbioses. *AsPT1* or *AsPT4* suppression showed decreased levels of total colonization and arbuscule development (Fig. 8), and led to premature death arbuscules. Silencing of *AsPT4* by RNAi resulted in a phenotype identical to the *MtPT4* mutants, suggesting that Pi delivery to the cortical cell by *AsPT4* might serve as a signal to permit continued development of the arbuscule and consequently to sustain proliferation of the fungus (Javot *et al.*, 2007a,b).

Symbiotic phosphate transport in AM *A. sinicus* was mediated by the specific phosphate transporter AsPT4 but not AsPT1. Loss of AsPT4 function resulted in a block in symbiotic Pi uptake, and knockdown of *AsPT1* also affected arbuscule morphology and growth of arbuscules of *G. intraradices*, surprisingly, did not alter Pi transfer in AM symbiosis, indicating compensatory effects between the two transporters. The AsPT1 do not compensate for the loss of the AsPT4, thereby showing that the functional establishment of the AM symbiosis enhanced the Pi status of *AsPT1* RNAi plants, but not of *AsPT4* RNAi genotypes. As observed in *A. sinicus*, in rice, mutations in the *Pht1;11* gene caused a decrease in symbiotic Pi uptake capacity of the mycorrhizal root that resulted in lower Pi content of shoot tissues, whereas *pht1;13* mutant plants did not affect this process (Yang *et al.*, 2012). The combined phenotypic and cellular localization analysis indicated that AsPT1 and AsPT4 play an indispensable role during the development of intraradical fungal structures, most prominently the arbuscules. It became apparent that AsPT1 and AsPT4 are not functionally redundant and no additive effect in AM symbiosis of *A. sinicus*.

AsPT1, probably encoding a transceptor, mediates Pi concentrations at the peribascular interface

The most intriguing study on the function of AM-specific AsPT1 originates from its distinctions from AsPT4. Although AsPT1 encodes a functional plasma membrane-localized transporter that mediates high-affinity Pi activity in yeast, and AsPT1 is required for arbuscule development in *A. sinicus*, AsPT1 is not necessary and sufficient to mediate the symbiotic Pi uptake. A higher level of *AsPT1* expression promoted the intraradical fungal development of *G. intraradices* and, interestingly, altered Pi transfer in mycorrhizal roots (Fig. 6). The results suggest that AsPT1 may moderately contribute to symbiotic Pi uptake in *A. sinicus*. So far, the detail function of AsPT1 protein at the peribascular interface is still unclear. It is probable that AsPT1 plays an important role in symbiotic signalling. Currently, the discovery of nutrient transceptors, transporter-like proteins with a receptor function, suggests that receptors for environmental signals may have been derived in evolution from nutrient transporters (Thevelein & Voordeckers, 2009). In rice, a symbiosis-specific OsPT13 protein was suggested to have a nontransporting transceptor role in symbiotic signalling affecting arbuscule development (Yang *et al.*, 2012). Therefore, AsPT1, a probable nutrient sensor protein with high transport activity, might have been discovered in *A. sinicus*. The synergism of AsPT1 and AsPT4 might permit continued development of the arbuscule and effective fungal symbiont. Altogether, the phenotypic analysis and evidence led us to assume that AsPT1 probably encodes a functional transceptor involving Pi concentrations at the peribascular interface.

Taken together, there also exists a second Pi-transporter AsPT1 indispensable for the development of AM symbiosis in dicots. AsPT4 but not AsPT1 is necessary and sufficient to mediate symbiotic Pi transfer. The conserved *cis*-acting elements mediate the mycorrhiza-activated AsPT1 and AsPT4. Future studies should further address the isolation and subsequent characterization of the *trans*-acting factors binding to *cis*-acting elements, and explore their potential interaction with other transcription factors. This will help to strengthen our understanding of the regulation during the establishment of the AM symbiosis. The data provide new insights into plant proteins required for AM symbiosis, phosphate transport and pave the way for the identification of novel regulation factors essential for AM symbiosis.

Acknowledgements

This work was supported by the National Natural Science Foundation of China (30870082, 30800001). We are very grateful to Dr Guohua Xu for kindly providing the yeast mutant strain MB192 and the expression vector 112A1NE, and for his support in the experiments with the complementation analysis. We would like to thank Professor Shiping Wang for providing the pDS1301 vector for the RNAi experiment, Professor Zhongming Zhang for providing strain K599 for the plant transformations, and Professor Hong Long and student Xiaoning Fan for supporting microscopic studies. We would also like to thank Dr Christina Baker and Dr Ton for revising the manuscript.

References

- Ai P, Sun S, Zhao J, Fan X, Xin W, Guo Q, Yu L, Shen Q, Wu P, Miller AJ. 2009. Two rice phosphate transporters, OsPht1;2 and OsPht1;6, have different functions and kinetic properties in uptake and translocation. *Plant Journal* 57: 798–809.
- Andriankaja A, Boisson-Dernier A, Frances L, Sauviac L, Jauneau A, Barker DG, Carvalho-Niebel F. 2007. AP2-ERF transcription factors mediate Nod factor-dependent *MtENOD11* activation in root hairs via a novel *cis*-regulatory motif. *Plant Cell* 19: 2866–2885.
- Boisson-Dernier A, Chabaud M, Garcia F, Bécard G, Rosenberg C, Barker DG. 2001. *Agrobacterium rhizogenes*-transformed roots of *Medicago truncatula* for the study of nitrogen-fixing and endomycorrhizal symbiotic associations. *Molecular Plant–Microbe Interactions* 14: 695–700.
- Bucher M. 2007. Functional biology of plant phosphate uptake at root and mycorrhiza interfaces. *New Phytologist* 173: 11–26.
- Bucher M, Rausch C, Daram P. 2001. Molecular and biochemical mechanisms of phosphorus uptake into plants. *Journal of Plant Nutrition and Soil Science* 164: 209–217.
- Chen A, Gu M, Sun S, Zhu L, Hong S, Xu G. 2011. Identification of two conserved *cis*-acting elements, MYCS and P1BS, involved in the regulation of mycorrhiza-activated phosphate transporters in eudicot species. *New Phytologist* 189: 1157–1169.
- Chen A, Hu J, Sun S, Xu G. 2007. Conservation and divergence of both phosphate- and mycorrhiza-regulated physiological responses and expression patterns of phosphate transporters in solanaceous species. *New Phytologist* 173: 817–831.
- Chu Z, Yuan M, Yao J, Ge X, Yuan B, Xu C, Li X, Fu B, Li Z, Bennetzen JL. 2006. Promoter mutations of an essential gene for pollen development result in disease resistance in rice. *Genes & Development* 20: 1250–1255.
- Daram P, Brunner S, Rausch C, Steiner C, Amrhein N, Bucher M. 1999. Pht2;1 encodes a low-affinity phosphate transporter from *Arabidopsis*. *Plant Cell* 11: 2153–2166.
- Denison RF, Kiers ET. 2011. Life histories of symbiotic rhizobia and mycorrhizal fungi. *Current Biology* 21: R775–R785.
- Dermatsev V, Weingarten-Baror C, Resnick N, Gadkar V, Winger S, Kolotilin I, Mayzlish-Gati E, Zilberstein A, Koltai H, Kapulnik Y. 2010. Microarray analysis and functional tests suggest the involvement of expansins in the early stages of symbiosis of the arbuscular mycorrhizal fungus *Glomus intraradices* on tomato (*Solanum lycopersicum*). *Molecular Plant Pathology* 11: 121–135.
- Drissner D, Kunze G, Callewaert N, Gehrig P, Tamasloukht MB, Boller T, Felix G, Amrhein N, Bucher M. 2007. Lyso-phosphatidylcholine is a signal in the arbuscular mycorrhizal symbiosis. *Science* 318: 265–268.
- Ezawa T, Cavagnaro TR, Smith SE, Smith FA, Ohtomo R. 2004. Rapid accumulation of polyphosphate in extraradical hyphae of an arbuscular mycorrhizal fungus as revealed by histochemistry and a polyphosphate kinase/luciferase system. *New Phytologist* 161: 387–392.
- Fehlberg V, Vieweg MF, Dohmann EMN, Hohnjec N, Pühler A, Perlick AM, Küster H. 2005. The promoter of the leghaemoglobin gene *vflb29*: functional analysis and identification of modules necessary for its activation in the infected cells of root nodules and in the arbuscule-containing cells of mycorrhizal roots. *Journal of Experimental Botany* 56: 799–806.
- Floss DS, Hause B, Lange PR, Küster H, Strack D, Walter MH. 2008. Knock-down of the MEP pathway isogene 1-deoxy-d-xylulose 5-phosphate synthase 2 inhibits formation of arbuscular mycorrhiza-induced apocarotenoids, and abolishes normal expression of mycorrhiza-specific plant marker genes. *Plant Journal* 56: 86–100.
- Frenzel A, Tiller N, Hause B, Krajinski F. 2006. The conserved arbuscular mycorrhiza-specific transcription of the secretory lectin *MtLec5* is mediated by a short upstream sequence containing specific protein binding sites. *Planta* 224: 792–800.
- Gomez-Ariza J, Balestrini R, Novero M, Bonfante P. 2009. Cell-specific gene expression of phosphate transporters in mycorrhizal tomato roots. *Biology and Fertility of Soils* 45: 845–853.
- Harrison MJ, Dewbre GR, Liu J. 2002. A phosphate transporter from *Medicago truncatula* involved in the acquisition of phosphate released by arbuscular mycorrhizal fungi. *Plant Cell* 14: 2413–2429.
- Hong J, Park YS, Bravo A, Bhattarai KK, Daniels DA, Harrison MJ. 2012. Diversity of morphology and function in arbuscular mycorrhizal symbioses in *Brachypodium distachyon*. *Planta* 236: 851–865.
- Javot H, Penmetsa RV, Terzaghi N, Cook DR, Harrison MJ. 2007a. A *Medicago truncatula* phosphate transporter indispensable for the arbuscular mycorrhizal symbiosis. *Proceedings of the National Academy of Sciences, USA* 104: 1720–1725.
- Javot H, Pumplin N, Harrison MJ. 2007b. Phosphate in the arbuscular mycorrhizal symbiosis: transport properties and regulatory roles. *Plant, Cell & Environment* 30: 310–322.
- Jia H, Ren H, Gu M, Zhao J, Sun S, Zhang X, Chen J, Wu P, Xu G. 2011. The phosphate transporter gene *OsPht1;8* is involved in phosphate homeostasis in rice. *Plant Physiology* 156: 1164–1175.
- Karandashov V, Bucher M. 2005. Symbiotic phosphate transport in arbuscular mycorrhizas. *Trends in Plant Science* 10: 22–29.
- Karandashov V, Nagy R, Wegmüller S, Amrhein N, Bucher M. 2004. Evolutionary conservation of a phosphate transporter in the arbuscular mycorrhizal symbiosis. *Proceedings of the National Academy of Sciences, USA* 101: 6285–6290.
- Kouchi H, Hata S. 1993. Isolation and characterization of novel nodulin cDNAs representing genes expressed at early stages of soybean nodule development. *Molecular & General Genetics* 238: 106–119.
- Li Y, Zhou L, Chen D, Tan X, Lei L, Zhou J. 2008. A nodule-specific plant cysteine proteinase, AsNODF32, is involved in nodule senescence and nitrogen fixation activity of the green manure legume *Astragalus sinicus*. *New Phytologist* 180: 185–192.
- Liu C, Muchhal US, Uthappa M, Kononowicz AK, Raghothama KG. 1998a. Tomato phosphate transporter genes are differentially regulated in plant tissues by phosphorus. *Plant Physiology* 116: 91–99.
- Liu F, Wang Z, Ren H, Shen C, Li Y, Ling HQ, Wu C, Lian X, Wu P. 2010. OsSPX1 suppresses the function of OsPHR2 in the regulation of expression of OsPT2 and phosphate homeostasis in shoots of rice. *Plant Journal* 62: 508–517.
- Liu H, Trieu AT, Blaylock LA, Harrison MJ. 1998b. Cloning and characterization of two phosphate transporters from *Medicago truncatula* roots: regulation in response to phosphate and to colonization by arbuscular mycorrhizal (AM) fungi. *Molecular Plant–Microbe Interactions* 11: 14–22.
- Liu Y-G, Chen Y. 2007. High-efficiency thermal asymmetric interlaced PCR for amplification of unknown flanking sequences. *BioTechniques* 43: 649–656.
- Loth-Pereda V, Orsini E, Courty PE, Lota F, Kohler A, Diss L, Blaudez D, Chalot M, Nehls U, Bucher M *et al.* 2011. Structure and expression profile of the phosphate Pht1 transporter gene family in mycorrhizal *Populus trichocarpa*. *Plant Physiology* 156: 2141–2154.
- Maeda D, Ashida K, Iguchi K, Chechetka SA, Hijikata A, Okusako Y, Deguchi Y, Izui K, Hata S. 2006. Knockdown of an arbuscular mycorrhiza-inducible phosphate transporter gene of *Lotus japonicus* suppresses mutualistic symbiosis. *Plant and Cell Physiology* 47: 807–817.
- Nagarajan VK, Jain A, Poling MD, Lewis AJ, Raghothama KG, Smith AP. 2011. *Arabidopsis* Pht1;5 mobilizes phosphate between source and sink organs and influences the interaction between phosphate homeostasis and ethylene signaling. *Plant Physiology* 156: 1149–1163.
- Nagy R, Karandashov V, Chague V, Kalinkevich K, Tamasloukht MB, Xu G, Jakobsen I, Levy AA, Amrhein N, Bucher M. 2005. The characterization of novel mycorrhiza-specific phosphate transporters from *Lycopersicon esculentum* and *Solanum tuberosum* uncovers functional redundancy in symbiotic phosphate transport in solanaceous species. *Plant Journal* 42: 236–250.
- Pao SS, Paulsen IT, Saier MH Jr. 1998. Major facilitator superfamily. *Microbiology and Molecular Biology Reviews* 62: 1–34.
- Paszowski U, Kroken S, Roux C, Briggs SP. 2002. Rice phosphate transporters include an evolutionarily divergent gene specifically activated in arbuscular mycorrhizal symbiosis. *Proceedings of the National Academy of Sciences, USA* 99: 13 324–13 329.
- Rae AL, Cybinski DH, Jarmey JM, Smith FW. 2003. Characterization of two phosphate transporters from barley; evidence for diverse function and kinetic properties among members of the Pht1 family. *Plant Molecular Biology* 53: 27–36.

- Rausch C, Daram P, Brunner S, Jansa J, Laloi M, Leggewie G, Amrhein N, Bucher M. 2001. A phosphate transporter expressed in arbuscule-containing cells in potato. *Nature* 414: 462–470.
- Reinders A, Schulze W, Kühn C, Barker L, Schulz A, Ward JM, Frommer WB. 2002. Protein-protein interactions between sucrose transporters of different affinities colocalized in the same enucleate sieve element. *The Plant Cell* 14: 1567–1577.
- Remy E, Cabrito TR, Batista RA, Teixeira MC, Sa'-Correia I, Duque P. 2012. The Pht1;9 and Pht1;8 transporters mediate inorganic phosphate acquisition by the *Arabidopsis thaliana* root during phosphorus starvation. *New Phytologist* 195: 356–371.
- Remy W, Taylor TN, Hass H, Kerp H. 1994. Four hundred-million-year-old vesicular arbuscular mycorrhizae. *Proceedings of the National Academy of Sciences, USA* 91: 11 841–11 843.
- Schaffer G, Peterson L. 1993. Modifications to clearing methods used in combination with vital staining of roots colonized with vesiculararbuscular mycorrhizal fungi. *Mycorrhiza* 4: 29–35.
- Scotto-Lavino E, Du GW, Frohman MA. 2006a. 5' end cDNA amplification using classic RACE. *Nature Protocols* 1: 2555–2562.
- Scotto-Lavino E, Du G, Frohman MA. 2006b. 3' end cDNA amplification using classic RACE. *Nature Protocols* 1: 2742–2745.
- Shin H, Shin HS, Chen R, Harrison MJ. 2006. Loss of *At4* function impacts phosphate distribution between the roots and the shoots during phosphate starvation. *Plant Journal* 45: 712–726.
- Shin H, Shin HS, Dewbre GR, Harrison MJ. 2004. Phosphate transport in *Arabidopsis*: Pht1;1 and Pht1;4 play a major role in phosphate acquisition from both low- and high- phosphate environments. *Plant Journal* 39: 629–642.
- Smith SE, Jakobsen I, Groenlund M, Smith FA. 2011. Roles of arbuscular mycorrhizas in plant phosphorus nutrition: interactions between pathways of phosphorus uptake in arbuscular mycorrhizal roots have important implications for understanding and manipulating plant phosphorus acquisition. *Plant Physiology* 156: 1050–1057.
- Smith SE, Read DJ. 2008. *Mycorrhizal symbiosis*. San Diego, CA, USA: Academic Press.
- Smith SE, Smith FA, Jakobsen I. 2003. Mycorrhizal fungi can dominate phosphate supply to plants irrespective of growth responses. *Plant Physiology* 133: 16–20.
- Sun S, Gu M, Cao Y, Huang X, Zhang X, Ai P, Zhao J, Fan X, Xu G. 2012. A constitutive expressed phosphate transporter, OsPht1;1, modulates phosphate uptake and translocation in phosphate-replete rice. *Plant Physiology* 159: 1571–1581.
- Tamura Y, Kobae Y, Mizuno T, Hata S. 2012. Identification and expression analysis of arbuscular mycorrhiza-inducible phosphate transporter genes of soybean. *Bioscience, Biotechnology, and Biochemistry* 76: 309–313.
- Tatsuhiko E, Sally ES. 2001. Differentiation of polyphosphate metabolism between the extra- and intraradical hyphae of arbuscular mycorrhizal fungi. *New Phytologist* 149: 555–563.
- Thevelein JM, Voordeckers K. 2009. Functioning and evolutionary significance of nutrient transceptors. *Molecular Biology and Evolution* 26: 2407–2414.
- Trouvelot A. 1986. Mesure du taux de mycorrhization VA d'un système racinaire. Recherche de méthodes d'estimation ayant une signification fonctionnelle. In: Gianinazzi-Pearson V, Gianinazzi S, eds. *Physiological and genetical aspects of Mycorrhizae*. Paris, France: INRA, 217–221.
- Wu Z, Zhao J, Gao R, Hu G, Gai J, Xu GH, Xing H. 2011. Molecular cloning, characterization and expression analysis of two members of the Pht1 family of phosphate transporters in *Glycine max*. *PLoS ONE* 6: e19752.
- Xu G, Chague V, Melamed-Bessudo C, Kapulnik Y, Jain A, Raghothama KG, Levy AA, Silber A. 2007. Functional characterization of LePT4: a phosphate transporter in tomato with mycorrhiza-enhanced expression. *Journal of Experimental Botany* 58: 2491–2501.
- Yang S, Grönlund M, Jakobsen I, Grottemeyer MS, Rentsch D, Miyao A, Hirochik H, Kumar CS, Sundaresan V, Salamin N *et al.* 2012. Nonredundant regulation of rice arbuscular mycorrhizal symbiosis by two members of the *PHOSPHATE TRANSPORTER1* gene family. *Plant Cell* 24: 4236–4251.
- Zhang Q, Blaylock LA, Harrison MJ. 2010. Two *Medicago truncatula* half-ABC transporters are essential for arbuscule development in arbuscular mycorrhizal symbiosis. *Plant Cell* 22: 1483–1497.

Supporting Information

Additional supporting information may be found in the online version of this article.

Fig. S1 Six members of the *Astralegus sinicus* PHT1 gene family.

Fig. S2 Deduced amino acid sequences of AsPT1 and Pht1 family of *A. sinicus* and legume.

Fig. S3 Hydrophobicity profiles calculated from the deduced amino acid sequences of AsPT1, AsPT2, AsPT3, AsPT4, AsPT5, and AsPT6.

Fig. S4 Putative *cis*-regulatory elements in the promoters of mycorrhiza-inducible Pht1 transporters and plant inorganic phosphate transporter genes from *A. sinicus* and other plant species.

Fig. S5 Spatial expression patterns of the Pht1 family genes in mycorrhizal *A. sinicus*.

Fig. S6 Subcellular localization of Pht1;1 and Pht1;4 transporters.

Fig. S7 Tissue localization analysis of *AsPT2*, *AsPT3* and *AsPT5*.

Fig. S8 Phosphate transport properties of AsPT5 in yeast.

Fig. S9 Polyphosphate staining of mycorrhizal control, *AsPT1* and *AsPT4* RNAi roots.

Table S1 Primers used in this study

Table S2 Accession numbers of the Pht1 family transporter

Methods S1 Detailed procedures.

Please note: Wiley-Blackwell are not responsible for the content or functionality of any supporting information supplied by the authors. Any queries (other than missing material) should be directed to the *New Phytologist* Central Office.